Waveform Modeling of Earthquake Data for Delineating the Sedimentary Structure of the Anchorage Basin, Alaska

U. Dutta[1], M. K. Sen[2], N. N. Biswas[3] and Z. Yang[4]

[1]*Department of Civil Engineering, University of Alaska Anchorage, 3211 Providence Dr., Anchorage, AK 99508, USA. Tel: (907) 786-1952, Fax: (907) 786-1079, Email: afud@uaa.alaska.edu.*

[2]*Jackson School of Geosciences, University of Texas at Austin, 10100 Burnet Road Building 196, TX 78758, USA, Tel: (512) 471-0466, Fax: (512) 471-8844, Email: mrinal@ig.utexas.edu*

[3] *Geophysical Institute, University of Alaska Fairbanks, PO BOX 757320, Fairbanks, AK 99775, USA. Tel: (907) 474-7373, Fax: (907) 474-7290, Email: ffnnb@uaf.edu*

[4] *Department of Civil Engineering, University of Alaska Anchorage, 3211 Providence Dr., Anchorage, AK 99508, USA. Tel: (907) 786-6431, Fax: (907) 786-1079, Email: afzy@uaa.alaska.edu.*

ABSTRACT:

The paper presents waveform inversion technique using the local earthquake data to estimate the crustal structure of the Anchorage basin, Alaska. Three component recorded data of an earthquake (M_L= 4.8) from 26 strong motion station sites in Anchorage area are used for this purpose. The technique uses parallelized reflectivity method to compute synthetic seismograms of SH-, SV-, and P- wave motions and implements global optimization technique based on simulated annealing inversion to fit the observed waveform data with the computed seismograms. The inversion searches for optimal values of four model parameters namely the layer thickness, P-wave velocity, P to S-wave velocity ratio and density at each site. The inversion shows that the crustal thickness of the Anchorage basin is around 40 km with P- and S-wave velocity at the bottom of the crust is around 6.4 km/s and 3.8 km/s, respectively. It is noticed that the observed ground motions of the Anchorage basin are strongly affected by the S-wave velocities of the shallow (< 0.1 km) sediments. The P-wave amplification due to the basin sediments is not significant. The presence of low S-wave velocity zones primarily responsible for the observed variations of the ground motions characteristics within the Anchorage basin. The P-to-S-wave velocity ratio varies from 10.0 to 2.0 for the shallower parts of the basin and remains around 1.78 in the deeper parts of the basin.

KEYWORDS: Waveform inversion, sedimentary basin, P and S-wave velocity, simulated annealing

1. INTRODUCTION

Anchorage is the largest population center in the State of Alaska and located in a highly active seismic zone of southcentral Alaska. In 1964, the area was widely damaged by the Prince William Sound earthquake (Mw=9.2), the second largest earthquake ever recorded in the world. A strong motion network consists of 40 free-field stations is currently operating in the metropolitan area of Anchorage. Several investigations have been conducted to study the site response (Dutta et al., 2001, Martirosyan et al., 2002, Dutta et al., 2003), seismic site classification (Dutta et al., 2000, Nath et al., 1997), and the attenuation characteristics (Dutta et al., 2004) of the shallow sediments of the basin. A strong correlation has observed between the spatial variation of site response and seismic site classes based on the uppermost 30 m shear wave velocity data as per NEHRP classification. Using the microtremor data, Dutta et al. (2007) estimated the S- wave velocity structure up to the depth of 1 km at nine sites of the basin and related the high frequency amplification of the Anchorage basin with the presence of low velocity sediments at relatively deeper depths. However, understanding of the seismic wave propagation through the crust and its interaction with the sedimentary basin is an important task to explain the observed spatial variation of the ground motion response in the Anchorage area.

In this paper, we present a waveform modeling technique and demonstrate its application to determine the crustal structure beneath the Anchorage area. The technique applies the reflectivity method (Kennett, 1983) to compute synthetic seismograms due to an earthquake and implements a global optimization algorithm using Very Fast Simulated Annealing (VFSA) (Ingber 1989; Sen & Stoffa, 1995) to invert for a 1-D sedimentary structure by comparing synthetic seismograms with the recorded time series data from twenty-six strong motion station sites of the Anchorage strong motion network.

2. GEOLOGIC AND TECTONIC SETUP

The geological formation of the Anchorage basin is dipping towards west and abutting on the metamorphic bedrock of the Chugach Mountains to the east (Figure 1). The thickness of the basin probably exceeds a few km, as the stratigraphic test hole (Romig Park No. 1) near the Campbell Lake (H in Figure 1) drilled to a depth of about 3.5 km failed to penetrate the bedrocks (Yehlee et al., 1986). The bedrock ranges in age from upper Paleozoic through upper Mesozoic. The thick deposits of the Tertiary sediments of non-marine origin (Updike and Ulery, 1986), principally composed of sandstone, siltstone and claystone immediately overlying the bedrock constitute the major unit of Cenozoic sequence beneath Anchorage lowlands. These in turn are overlain by several hundred meters of Quaternary deposits (Schmoll and Barnwell, 1984) from widespread Pleistocene glacial advances into the lowlands from the surrounding ranges. The Bootlegger cove formation (BCF) constitutes one of the important Quaternary deposits, mainly underlie towards the western parts of Anchorage and its downtown area. The cohesive facies of BCF (Updike and Ulery, 1986) consisting of silty clay and/or clayey silt are susceptible to liquefaction and caused extensive ground failure during the 1964 Prince William Sound earthquake. The non-cohesive facies, on the other hand, consist of silt and fine sand. Overlying the BCF are outwash/landslide deposits, which attain several meters in thickness in some parts of the Anchorage basin (Combellick, 1999).

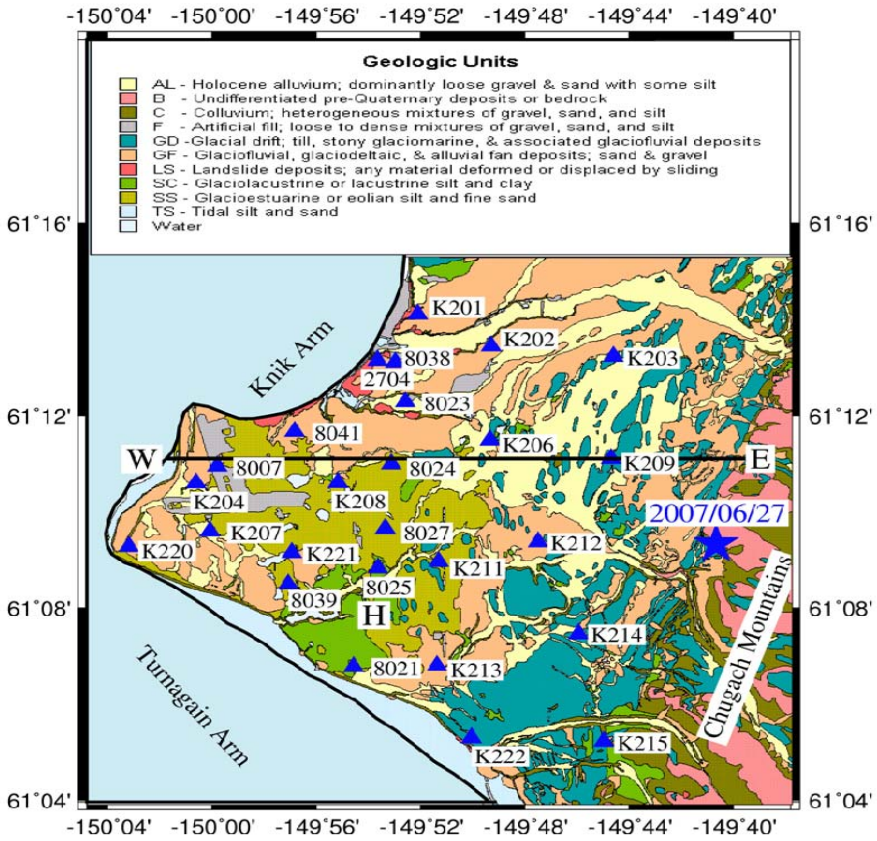

Figure 1: The location of the strong motion stations (triangle) and the epicenter of the earthquake (star) used for the present analysis are plotted on the background of the geological map of the area (Combellick, 1999)

3. DATA AND DATA PROCESSING

Three component recorded ground motion data from twenty-six station sites of Anchorage strong motion network has been considered for the analysis (Figure 1). Each station is equipped with a three-component accelerograph (K2 of Kinemetrics Inc.) and the data are recorded at 200 samples per second. The sensors are operated under triggered

mode with 1 gal threshold level with pre-event and post-event triggered duration of 30 and 80 sec, respectively. The recorded ground motion data are first band-pass filtered between 0.01-5.0 Hz. The horizontal components of the filtered dataset are rotated along the radial and transverse direction to obtain the ground motion response due to SV- and SH-wave, respectively. A time window of 25 sec starting from the origin time of the earthquake has been selected from all three components for the present analysis. This data window includes both the direct P- and S-wave arrivals as well as the later arrivals at each site.

The epicenter of the event is located near the foothills of the Chugach Mountains in the eastern part of the Anchorage area (Figure 1). The moment tensor solution of the recorded event and its hypocentral parameters are taken from the Alaska earthquake Information Center (AEIC) database (Table 1).

4. WAVEFORM MODELING

The waveform modeling technique presented here is an implementation of the reflectivity method (Kennett 1983; Mallick & Frazer, 1987) with a global optimization algorithm (Sen & Stoffa, 1991; 1995). For a given

Table 1: Hypocentral parameters and the Moment tensor solution of the event (AEIC)

Date & Origin Time (UTC)	Location			Moment Tensor Parameters (xE+23)						
	Longitude (^{o}W)	Latitude (^{o}N)	Depth (km)	M_o	M_{xx}	M_{xy}	M_{xz}	M_{yy}	M_{yz}	M_{zz}
2006/06/27 13:18:01.00	-149.6776	61.1554	36.0	1.34	-0.13	-0.67	-0.47	1.13	-0.15	-1.00

source depth and epicentral distance, the method computes reflectivity matrices for a stack of 1-D layers as a function of ray parameters and angular frequencies and produces all possible seismic phases. The reflectivity responses for different ray parameters and frequencies are computed completely independent to each other. For this study, sixteen parallel processors system is used to distribute these ray parameter computations, and message passing therein, using the Message Passage Interface (MPI) Standard (Gropp and Lusk, 1995), to communicate between these processors and to assemble the individual responses. Finally, an inverse transformation from ray parameter domain to a plane wave offset domain is applied to generate synthetic seismograms at the required azimuths and distances from the source location.

The objective of the study is to estimate the model parameters e.g., P-wave velocity, the P-and S-wave velocity ratio (Vp/Vs), thickness and density that produce synthetic waveforms for a given source–receiver which fits best with the observed record in terms of *l*-2 norm criterion. The combined cross-correlation between vertical, radial and transverse component of the data with the computed P-, SV- and SH- synthetics, respectively in a specified time window (25 sec) is used to set this criterion. The error function, E(**m**) for any given set of model parameters, **m**, is defined as the negative of the cross correlation (Sen and Stoffa, 1991) and it is given by

$$E(\mathbf{m}) = -2\left[(\mathbf{O}_v \bullet \mathbf{S}_v)/\{|\mathbf{O}_v| + |\mathbf{S}_v|\} + (\mathbf{O}_r \bullet \mathbf{S}_r)/\{|\mathbf{O}_r| + |\mathbf{S}_r|\} + (\mathbf{O}_t \bullet \mathbf{S}_t)/\{|\mathbf{O}_t| + |\mathbf{S}_t|\}\right] \quad (1)$$

where (O_v, S_v) , (O_r, S_r) and (O_t, S_t) represent the vertical, radial and transverse components of the observed and computed synthetic seismograms, respectively, and |.| indicates the *l*-2 norm.

The global optimization algorithm based on the simulated annealing (SA) method has been adopted as an inversion tool for the present analysis. The inversion with SA technique begins with an initial model $\mathbf{m_0}$ with associated error E ($\mathbf{m}_0$) between the observed and synthetic data computed based on Equation (1). During the process of iteration, it draws new model, $\mathbf{m}_{new}$, from a flat distribution of models with the predefined limits. The associated error function of the new model E ($\mathbf{m}_{new}$) is then computed and compared with E ($\mathbf{m}_0$). If E ($\mathbf{m}_{new}$) < E ($\mathbf{m}_0$), then $\mathbf{m_{new}}$ is accepted unconditionally and replaces $\mathbf{m_0}$. However, if E ($\mathbf{m}_{new}$) > E ($\mathbf{m}_0$), then $\mathbf{m}_{new}$ is still accepted with a probability of exp (-[E($\mathbf{m}_{new}$)-E($\mathbf{m}_0$)]/T) where T is a control parameter, known as annealing temperature, that controls the entire search process (Sen, 2006). This completes one iteration of the inversion. The rule of accepting new model with a probability makes it possible for SA to jump out of the local minima. Such generation-acceptance process is repeated several times at a particular constant temperature, T, and then T is lowered according to a predefined cooling schedule and the process is repeated again. With fast cooling, the algorithm will be trapped in local minimum while slow cooling takes a long time but it will reach the global minimum. Hence, there is a trade-off between the accuracy and computational cost. The algorithm is stopped when the error does not change after a sufficient number of trials. The parameter T controls the inversion; typically, T is set at a very high value (0.01) at the initial stage of iteration and gradually lowered as the inversion progresses until it reaches around 10^{-21}. Kirkpatrick *et al.* (1983) first introduced SA as a tool for the non-linear geophysical inversion. Sen and Stoffa (1991) demonstrated the applicability of SA to seismic waveform inversion.

To perform faster search of the model space than the classical SA, without sacrificing the solution, a variant of SA called very fast simulated annealing (VFSA) based on Ingber (1989) has been used in present waveform inversion technique. In VFSA, the new models are drawn from a temperature-dependent Cauchy-like distribution centered on the current model. This has two fundamental advantages. First, it provides a larger sampling of the model space at the early stages of the waveform inversion when T is high and much narrower sampling as the inversion converges and temperature decreases. Second, each model parameters can have its own individual cooling schedule and model-space perturbation based on their *a priori* information (Sen and Stoffa, 1995; Sen, 2006).

4.1 Uncertainty Estimation

The inversion performed several thousands of iterations (3000); thus thousands of models and associated error function (E ($\mathbf{m}$)) for each model were calculated. Due to non-uniqueness properties of the geophysical inverse problem, the error functions are either multi-valued or have broad minima. The VFSA searches the model space efficiently to identify the range of models that fit the data. The products of multiple such searches provide the uncertainty in a single, best-fitting solution. Such evaluation is necessary in seismic waveform modeling because more than one model can often explain the observed data equally well and trade-offs between different model parameters are common.

To evaluate the uniqueness and physical feasibility of the resulting model obtained from the waveform inversion, marginal posterior probability density (PPD) function using the Bayesian statistics (Tarantola,1987), and several other statistical measures e.g., variance and correlation (Sen and Stoffa, 1996). While the variance gives the measure of the spread about the mean and thus provides the variability of each individual parameter, the correlation of one parameter with all other parameters reflects the ambiguities of interpretation. Sen and Stoffa (1996) examined several different approaches for conducting the sampling of the model space and concluded that multiple-VFSA based approach, though theoretically approximate produces efficient sampling of the model space. In multiple VFSA, the VFSA algorithm runs for several run (10 in this study) with different starting models to allow the sufficient sampling of the entire model space and thus minimizes the biases in PPD. This will improve the estimates of the model covariance matrix and can also save several orders of magnitudes in the number of model evaluation over other methods.

5. RESULTS AND INTERPRETATIONS

In order to delineate the crustal structure of the Anchorage basin, we assumed a 16-layered 1-D earth model at each site. The main task of the inversion is to assign proper search limits for individual model parameters so that a realistic 1-D model can be obtained. The bound imposed on the P-wave velocity (V_P) at the deeper parts (> 0.1 m) of the basin is based on Frankel (2004) and 1-D velocity model routinely used by the AEIC for locating earthquakes in southcentral Alaska. However, no prior information of V_P for the shallow sediments (< 0.1 km) of the Anchorage basin is available. We therefore assumed the V_P to vary between 0.5 km/sec to 2.5 km/sec based on the results of obtained by Bonilla et al. (2002) for the Southern California area. To understand the effect of the near surface sediments on the observed ground motion characteristics, the maximum and minimum value of the layer thicknesses are assigned in such a way that the uppermost 100 meters of the basin are represented by the top 10 layers while the remaining six layers represent the structure between 100 m to 60 km. We have considered the V_P/V_S ratio (R) as the model parameters instead of searching directly for S-wave velocity. The S-wave velocity for each layer is however computed in each step for reflectivity computation from the V_p and R values. To constrain the R-values, we assumed it to vary between 1.7 to 12.0 for the shallow sediments and 1.7 to 2.0 for the deeper parts of the basin. A constant frequency independent attenuations of P- (Q_p) and S-wave (Q_s) for each layer is assumed with $Q_p = 2Q_s$. To represent highly attenuating near surface sediments, Q_s is assumed to vary gradually from 30 for the shallow sedimentary section to 250 at the bottom of the crust. The densities for shallow sediments are assumed to vary

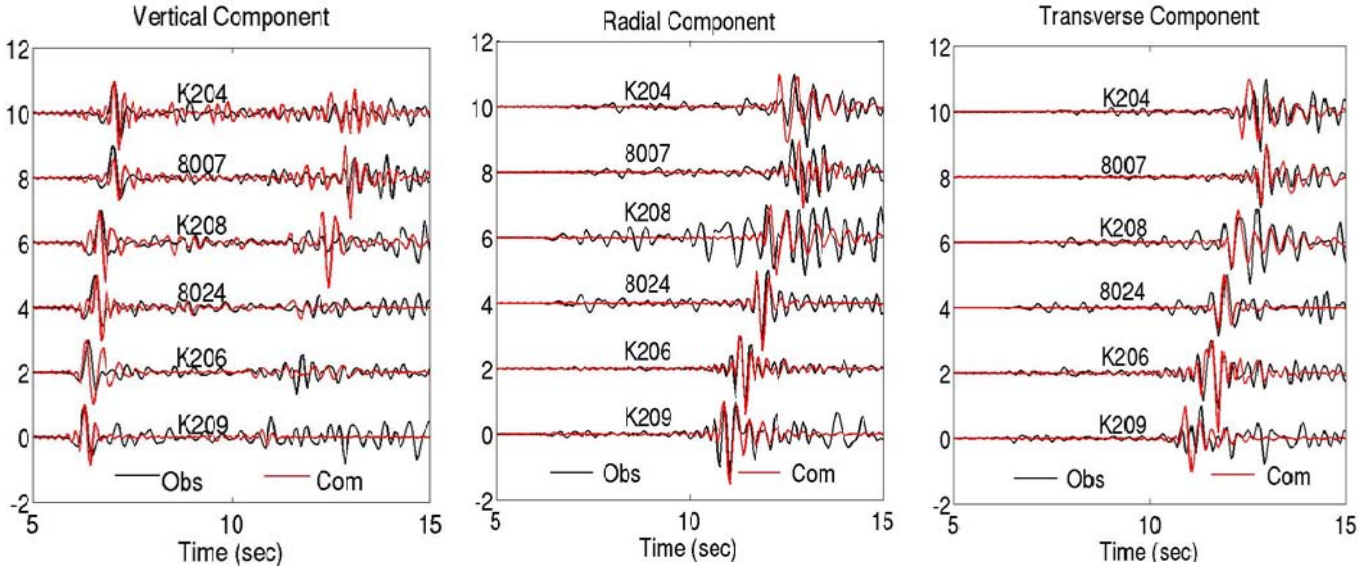

Figure 2: The comparison of the observed (black line) and computed seismograms at six sites located along the EW line of the Figure 1.

between 1.8 to 2.4 gm/cc, while for the deeper sediments they vary between 2.5 to 3.0 gm/cc.

With the above pre-defined limit imposed on the model parameters, the inversion of three components acceleration data has been carried out individually for each site. The inversion searches for the optimal 1-D layered earth model for each site that explain the observed data. Figure 2 shows as an example, the comparison between the observed and computed response for three components (vertical, radial and transverse) data for 5-15 sec time interval from the origin time for the mean model obtained from inversion at six sites in the Anchorage basin. It indicates that the model obtained from the inversion reasonably explain the observed data. Figure 3 shows the mean model for P and S-wave velocity from inversion for above six sites as indicated in each plot. The models indicate that the average crustal thickness of the basin is around 40 km and the P- and S-wave velocity increase gradually from surface to crust-mantle boundary and the average value at the lower crust is around 6.4 km/s and 3.8 km/s, respectively. No significant variation of overall crustal structure has been observed for sites from the eastern to western parts of the

basin. Figure 3 shows the P- and S-wave velocity variation for the uppermost 100 m of the Anchorage basin. It clearly shows the velocity structure changes significantly at the shallower parts of the basin. The model indicates that the S-wave velocity in uppermost 20 m is around 200-300 m/s at the western and central parts of the basin and increases to 350 m/s to 400 m/s at the eastern parts of the basin close to the Chugach Mountains. However, at the western side (K204, 8007 and K208) of the basin, the depth of the engineering bedrock with S-wave velocity

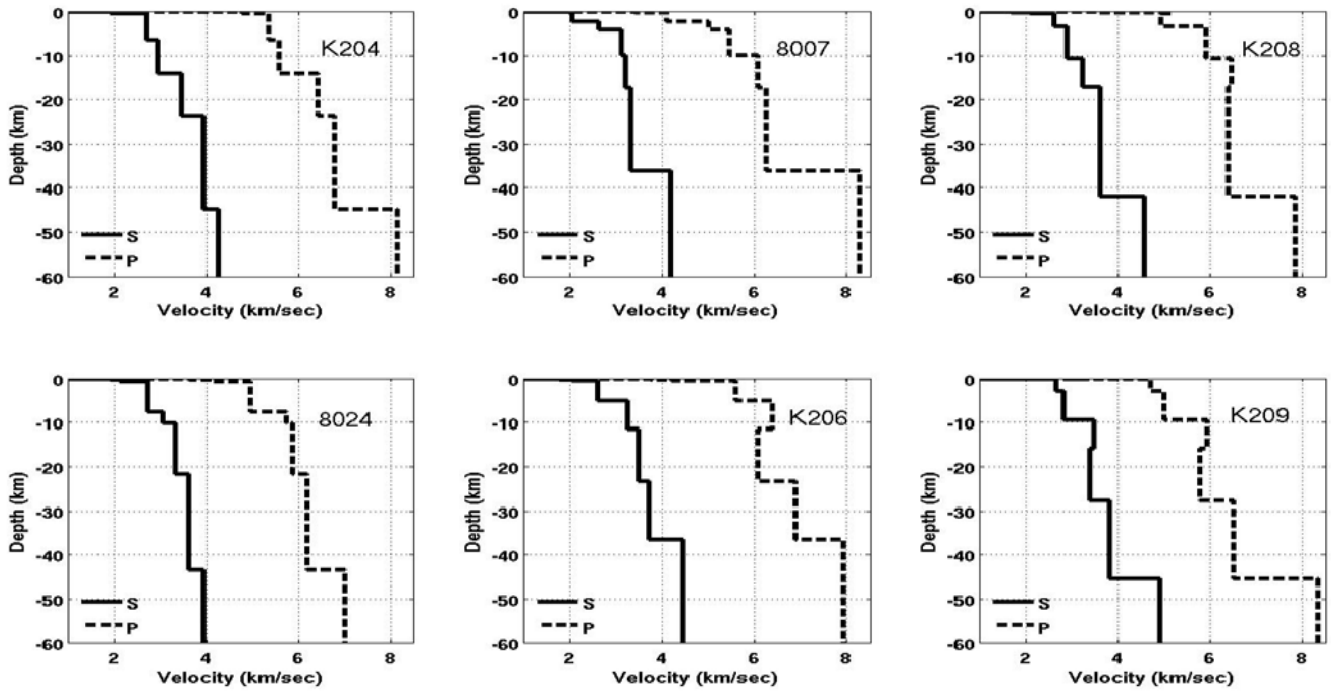

Figure 3. The P- (dashed line) and S-(solid line) wave velocity models for six sites in the Anchorage basin. The site names are marked at the right hand corner of each plot and the site locations are provided in Figure 1.

approximately 700-800 m/s is around 22 to 25 m which increases to around 60 m at the central parts of the basin (8024) and gradually decreases to 25 m at the eastern side (K209) of the basin. The models in Figure 3 also indicate a high Vp/Vs ratio (~ 4-10) for the uppermost 60-70 m of the basin, due to the presence of highly saturated sediments. The ratio reduces to around 2-2.5 around 100 m.

5. CONCLUSIONS

We describe the waveform modeling techniques based on the parallelized reflectivity method to compute the synthetic seismograms and apply the global optimization algorithm using VFSA to provide optimal model parameters to delineate the P- and S-wave velocity structure underneath the sites. The method has special advantageous in a sense that it can model simultaneously all the phases that might be present in the observed waveform and independent estimate both P-and S-wave velocity structure. The method successfully delineates the crustal structure of the Anchorage basin and the model obtained from the inversion appears to be consistent with the results obtained earlier. The variation of ground motion as observed in the Anchorage basin for frequency band 0.01-5.0 Hz is mainly due to the variation of the velocity structure of sediments from the uppermost few hundreds of meters. The P-wave amplification due to shallow sediments is not appearing to be significant in the Anchorage basin.

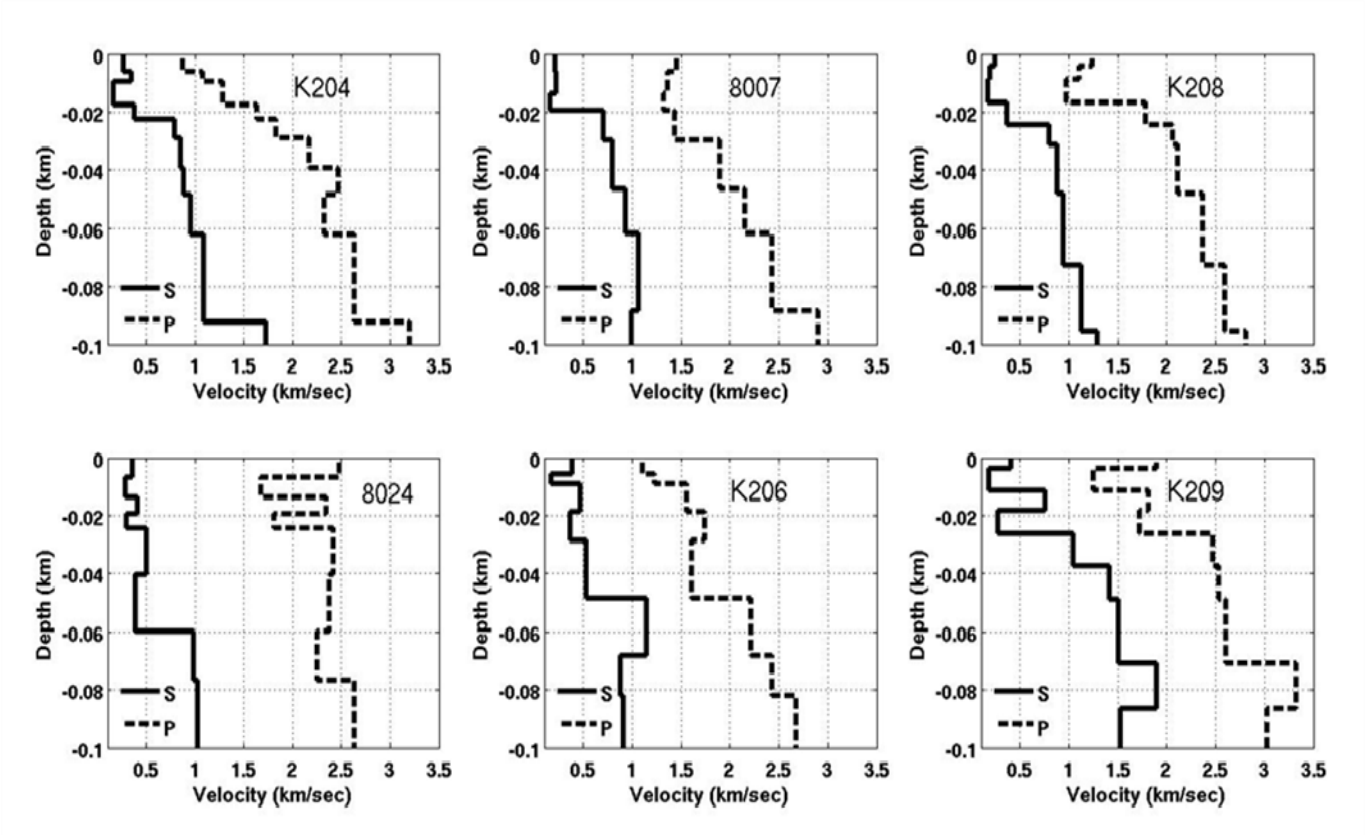

Figure 4. The P- (dashed line) and S-(solid line) wave velocity structure for shallow sediments at six sites of the Anchorage basin. The site names are marked at the right hand corner of each plot and the site locations are provided in Figure 1.

6. ACKNOWLEDGEMENTS

We thankfully acknowledge the partial research support received from the Chancellor's Fund of the University of Alaska Anchorage to carry out this work.

REFERENCES

Bonilla, L. F., J.H. Steidl, J.C. Gariel and R.J. Archuleta (2002). Borehole response studies at the Garner valley downhole array, Southern California, *Bull. Seism. Soc. Am.* **92**, 3165–3179.

Combellick, R. (1999). Simplified geologic map and cross sections of central and east Anchorage, Alaska, Preliminary Interpretive report 1999- 1, Alaska Division of Geology and Geophysical Surveys, Fairbanks, Alaska, scale 1:25,000.

Dutta, U., N. Biswas, A. Martirosyan, S. Nath, M. Dravinski, A. Papageorgiou, and R. Combellick (2000). Delineation of spatial variation of shear wave velocity with high frequency Rayleigh waves in Anchorage, Alaska, *Geophys. J. Int.* **143**, 365-375.

Dutta, U., A. Martirosyan, N. Biswas, A. Papageorgiou, M. Dravinski, and R. Combellick (2001). Estimation of S-wave site response in Anchorage, Alaska, from weak motion data using generalized inversion method, *Bull. Seism. Soc. Am.* **91**, 335–346.

Dutta, U., N. Biswas, A. Martirosyan, A. Papageorgiou, and S. Kinoshita (2003). Estimation of earthquake source parameters and site response in Anchorage, Alaska from strong motion network data using generalized inversion method, *Phys. Earth Planet. Interiors* **137,** 13–29.

Dutta, U., N. Biswas, D. Adams, A. Martirosyan, A. Papageorgiou (2004). Analysis of S-wave attenuation in southcentral Alaska, *Bull. Seism. Soc. Am.* **94,** 16-28**.**

Dutta, U., T. Satoh, H. Kawase, T. Sato, N. Biswas, A. Martirosyan, and M. Dravinski (2007). S-wave velocity structure of sediments in Anchorage, Alaska estimated with array measurements of microtremors, *Bull. Seism. Soc. Am.* **97**, 234-255.

Frankel, A. (2004). Rupture process of the M7.9 Denali fault Alaska earthquake: subevents, directivity, and scaling of high frequency ground motions, *Bull. Seism. Soc. Am.* **94**, S234-S255.

Gropp, W., and E. Lusk (1995). Dynamic process management in an MPI setting, *7th IEEE Symposium on Parallel and Distributeed Processing*, p.530

Ingber, L. (1989). Very fast simulated reannealing, *Mathematical Computer Modeling* **12**, 967-993.

Kennett, B.L.N. (1983). *SeismicWave Propagation in Stratified Media*, Cambridge University Press, Cambridge, 338 pp.

Kirkpatrick, S. G., C. D. Delatt Jr. and M. P. Vecchi (1983). Optimization by simulated annealing, *Science* **220**, 671-680.

Martirosyan, A., U. Dutta, N. Biswas, A. Papageorgiou, and R. Combellick (2002). Determination of site response in Anchorage, Alaska on the basis of spectral ratio methods, *Earthq. Spectra* **18**, 85-104.

Mallick, S. and L.N. Frazer (1987). Practical aspects of reflectivity modeling, *Geophysics*, **52,** 1355–1364.

Meteropolis, N., A. Rosenbluth, M.Rosenbluth, A. Teller (1953). Equation of state calculations by fast computing machines, *J. Chem. Phys.* **21**, 1087-1092.

Nath, S. K., D. Chatterjee, N. N. Biswas, M. Dravinski, D. A. Cole, A. Papageorgiou, J. A. Rodriguez, and C. J. Poran (1997). Correlation study of shear wave velocity in near surface geological formations in Anchorage, Alaska, *Earthq. Spectra* **13**, 55-75.

Schmoll, H. R., and W. W. Barnwell (1984). East-west geologic crosssection along DeBarrline, Anchorage, Alaska, *U.S. Geol. Surv. Open- File Rep. 84-791*, 10 pp., scale 1:28,000.

Sen, M. K**.** and P. L. Stoffa (1991). Non-linear one-dimensional seismic waveform inversion using simulated annealing, *Geophysics* **56**, 1624-1638.

Sen, M. K. and P. L. Stoffa (1995). Global Optimization methods in geophysical inversion, *Elsevier Science Publ. Co*.

Sen, M. K. and P. L. Stoffa (1996). Bayesian inference, Gibbs sampler and uncertainty estimation in geophysical inversion, *Geophy. Prosp.* **44**, 313-350.

Sen, M. K (2006). Seismic Inversion, *Society of Petroleum Engineers*, Richardson, TX, USA.

Tarantola, A. (1987). Inverse Problem Theory, Methods of Data Fitting and Model Parameter Estimation, *Elsevier Science Publ. Co*.

Updike, R. G., and C. A. Ulery (1986). Engineering geologic map of Southwest Anchorage, Alaska, Report No. 89, *Alaska Division of Geology and Geophysical Surveys*, Fairbanks, AK.

Yehle, L. A., J. K. Odom, H. R. Schmoll, and L. L. Dearborn (1986). Overview of the geology and geophysics of the Tikishla Park drillhole, U.S.G.S. A-84-1, Anchorage, Alaska, *U.S. Geological Survey Open-File Rep*., 86-293.